A Comparison Study of Nonlinear Solvers in Transient Circuit Analysis Involving Power Diodes

Ming Chen, Xiaoping Sun, Yanmei Zhang, He Chen, Pengcheng Zhu, and Jiawei Wang

Abstract The power diode is one of the most widely adopted devices in power electronics, thus intensive efforts has been made to reveal the underlying mechanism of its complex nonlinear behavior and develop reliable modeling and simulation methods. Existing circuit analysis tools often adopt implicit time integration methods such as the well-known backward Euler method, thus are faced with the solutions to nonlinear algebraic equations arising from time discretization. for large systems involving thousands of diodes and other semiconductor devices, e.g., the high voltage direct current (HVDC) transmission systems, the computational overheads can be prohibitive. In this manuscript, we focus on sorting out the most efficient nonlinear solver for tackling the nonlinearity of a single diode. Both Newton-type and fixed-point solvers are tested. Numerical results indicate that Newton-type solvers are more robust, while fixed-point solvers may be more efficient under small time-step size. This conclusion should shed light on the choice of sub-solvers in decomposition-like algorithms for transient analysis of practical large-scale power electronics.

Keywords Fixed-point method · Jacobian-free Newton-Krylov methods · Power diodes · Transient analysis

M. Chen
Ultra High Voltage Transmission Company of China Southern Power Grid Co., Ltd., Guangzhou 510663, China

X. Sun · Y. Zhang · H. Chen
Xi'an Xidian Power System Co., Ltd., Xi'an 710118, China

X. Sun · P. Zhu · J. Wang (✉)
School of Electrical Engineering, Xi'an Jiaotong University, Xi'an 710049, China
e-mail: jwwang@xjtu.edu.cn

X. Dong et al. (eds.), *The proceedings of the 10th Frontier Academic Forum of Electrical Engineering (FAFEE2022)*, Lecture Notes in Electrical Engineering 1054,
https://doi.org/10.1007/978-981-99-3408-9_54

1 Introduction

The power diode [1] may be one of the most widely adopted devices in power electronics, thus intensive efforts has been made to reveal the underlying mechanism of the complex nonlinear behavior of the diodes and develop reliable modeling methods. Existing models of power diodes can be roughly divided into system-level models and device-level models. System-level models, which approximate the diodes' behavior by multi-value resistors and ideal switches, are favorable for low computational overheads, while the accuracy is not satisfying for many scenarios, e.g., loss calculation and electromagnetic interference (EMI) evaluation [2]. Device-level models, either behavior-based or physics-based, take into account many physical phenomena, including emitter recombination, mobile charge carriers in depletion layer, and carrier multiplication, exhibit much more precise transient behavior than those of the system-level models.

However, popular circuit simulation tools, e.g., PSPICE, Matlab Simulink, and ANSYS Simplorer, often adopt implicit time integration methods, among which the backward Euler (BE) method may be the most common choice, are faced with the solutions to nonlinear algebraic equations arising from time discretization. For small problems involving only a few diodes, the dimensions of the nonlinear systems are limited, and the computational overheads are not a big issue. On the contrary, for large systems, e.g., the high voltage direct current (HVDC) transmission systems [3], thousands of diodes and other semiconductor devices are involved. The resultant dimensions of the nonlinear equations can be huge and bring up prohibitive computational costs.

Therefore, for large-scale transient analysis, decomposition-like techniques, including the latency insertion method (LIM) [4] and transmission-line links [5], are often used to decouple and analyze the whole system in a divide-and-conquer manner. In these techniques, the sub-solvers that can efficiently resolve the nonlinearity of a single component are essential for overall efficiency. Thus, in this manuscript, we focus on sorting out the most efficient nonlinear solver for tackling the nonlinearity of a single diode. Most existing nonlinear solvers fall into fixed-point methods or Newton methods. In this work, both types of nonlinear solvers are tested on a behavior-based diode model integrated in ANSYS Simplorer and comparison regarding convergence and efficiency are carried out.

2 Formulations

2.1 Behavior-Based Model of Diodes

The adopted model [6–8], which is a behavior-based dynamic model of power diodes integrated in ANSYS Simplorer, is presented in Fig. 1. The diode core of this model is described as

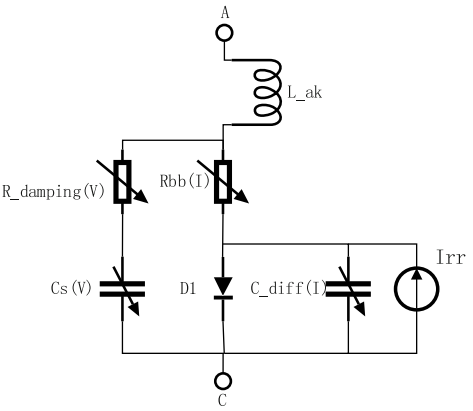

Fig. 1 Behavior-based dynamic model of diodes in ANSYS Simplorer

$$V_F = \frac{kT}{q} \ln\left(\frac{I_F}{I_S} + 1\right) + I_F \cdot R_B(I_F) \tag{1}$$

$$R_B(I_F) = \frac{R_B^0}{\sqrt{1 + I_D / I_{NOM}}} \tag{2}$$

where $k = 1.380649 \times 10^{-23}$ J/K is Boltzmann constant, $q = 1.602177 \times 10^{-19}$ C the elementary charge, T the temperature in Kelvin, and I_S the saturation current.

In addition to the static behavior modelled by the diode core, charging and discharging of junction and diffusion capacitance are taken into account by introducing voltage-dependent capacitances. There is a distinction between the evaluation of depletion and enhancement capacitance behavior, but the curves keep differentiable at the transition from one region to the other. The transition happens when the effective junction voltage

$$V_{PN} = V_C - VSHIFT\_JNCT \tag{3}$$

crosses 0 V. The voltage-dependent capacitances are given by the following piecewise function

$$C_S(V_{PN}) = \begin{cases} C_0 \cdot [2 - e^{-\frac{V_N}{V_{\text{diff}}}})], & V_{PN} \geq 0 \\ C_0 \cdot (\delta - \frac{1-\delta}{(1-\frac{V_{PN}}{V_{\text{diff}}})^{\alpha}}), & V_{PN} < 0 \end{cases} \tag{4}$$

where

$$V_N = \frac{V_{diff}}{(1-\delta) \cdot \alpha} \tag{5}$$

It's worth noting that to avoid possible oscillations, we involve a damping resistor $R_{DAMP} = DAMPING \cdot \sqrt{L/C}$, which is related to parasitic inductances as well as the internal capacitance.

The reverse recovery behavior is described by a controlled current source, i.e., I_{rr} in Fig. 1. The reverse recovery waveform and related shape parameters are presented in Fig. 2. The piecewise analytical formulations of the reverse recovery current are

$$I_{rr}(t) = \begin{cases} \frac{I_{rr\,\max}}{\exp\left(\frac{t_S}{TAU}\right)-1}\left[\exp\left(\frac{t}{TAU}\right)-1\right] & [0, t_B] \\ I_{rr\,\max}\sin(\omega_1 t + \varphi_1) & [t_B, t_S] \\ I_{rr\,\max}\cos(\omega_2 t + \varphi_2) & [t_S, t_C] \\ \frac{(R_3-R_2)I_{rr\,\max}}{SF_2 \cdot t_S} t + I_{rr\,\max}\left(R_2 - \frac{R_3-R_2}{SF_2 \cdot t_S} t_C\right) & [t_C, t_C + SF_2 \cdot t_S] \\ a(t - t_{end})^2 & [t_C + SF_2 \cdot t_S, t_{end}] \end{cases} \tag{6}$$

where the unknown coefficients are calculated as

$$\begin{cases} t_B = TAU \cdot \ln\left(R_1\left(\exp\left(\frac{t_S}{TAU}\right)-1\right)+1\right) \\ \omega_1 = \frac{\arcsin(R_1)-\frac{\pi}{2}}{t_B - t_s} \\ \varphi_1 = \frac{\pi}{2} - \frac{\arcsin(R_1)-\frac{\pi}{2}}{t_B - t_s} t_s \\ t_C = t_S(1 + SF_1) \\ \omega_2 = \frac{\arccos(R_2)}{SF_1 \cdot t_S} \\ \varphi_2 = -\frac{\arccos(R_2)}{SF_1} \\ t_{end} = t_C + SF_2 \cdot t_S - \frac{2R_3 \cdot SF_2 \cdot t_S}{R_3 - R_2} \\ a = \frac{R_3 \cdot I_{rr\,\max}}{(t_C + SF_2 \cdot t_S - t_{end})^2} \end{cases} \tag{7}$$

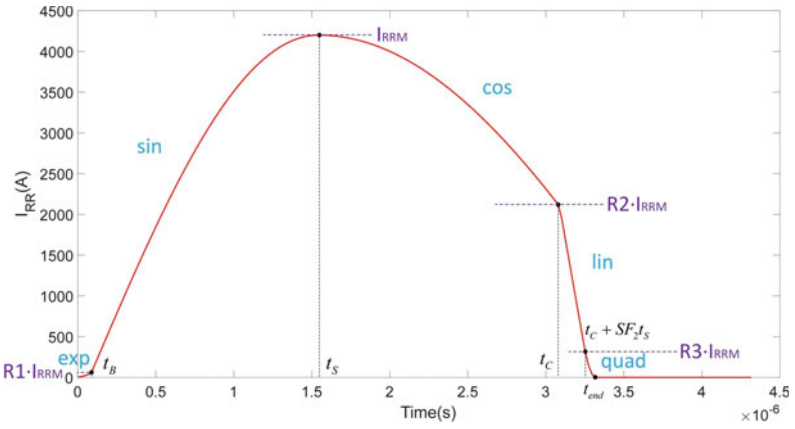

Fig. 2 Reverse recovery waveform and shape parameters

The unknown parameters in the above equations and figures can all be extracted by inputting the data from the manufacturer's datasheet into the modelling tool integrated in ANSYS Simplorer.

2.2 *Time Discretization of a Reference Problem*

The test model, which is the reference problem considered in our context, is depicted in Fig. 3. The governing equations of this model are

$$\begin{cases} \frac{dV_{ai}}{dt} = \frac{1}{R_{bb}C_{diff}}[V_{am} - V_{ai} - R_{bb}(I_F - I_{rr})] \\ \frac{dI_T}{dt} = \frac{1}{L_{ak}}(V_a - V_{am}) \\ \frac{du_{Cs}}{dt} = \frac{1}{R_{damping} \cdot C_S}(V_{am} - u_{cs}) \end{cases} \tag{8}$$

where the intermediate variables

$$\begin{cases} V_{am} = \left(I_T - \frac{V_{am}-u_{cs}}{R_{damping}}\right)R_{bb} + V_{ai} \\ I_F = I_S\left[\exp\left(\frac{qV_{ai}}{kT}\right) - 1\right] \\ R_{bb} = \frac{R_{B0}}{\sqrt{\frac{I_F}{I_{NOM}}+1}} \\ R_{damping} = DAMPING\sqrt{\frac{L_{ak}}{C_S}} \\ C_{diff} = TAU\frac{I_F+I_S}{M_0 \cdot \frac{kT}{q}} \\ C_S^{n+1} = \begin{cases} C_0 \cdot [2 - e^{-\frac{V_N}{V_{\text{diff}}}})], & V_{PN} \geq 0 \\ C_0 \cdot (\delta - \frac{1-\delta}{(1-\frac{V_{PN}}{V_{\text{diff}}})^\alpha}), & V_{PN} < 0 \end{cases} \end{cases} \tag{9}$$

The differential-algebraic equations (DAEs) given by Eqs. (8) and (9) are discretized by the widely adopted backward Euler (BE) scheme, which is unconditionally stable and can suppress unphysical oscillations of the numerical solutions. The resultant discretized DAEs are

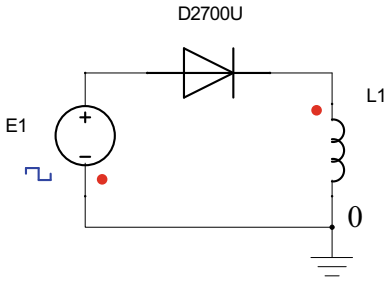

Fig. 3 The reference model

$$
\begin{cases}
V_{ai}^{n+1}\left(\frac{1}{\Delta t}+\frac{1}{R_{bb}^{n+1}C_{diff}^{n+1}}\right)-V_{ai}^{n}\left(\frac{1}{\Delta t}\right)-\frac{1}{R_{bb}^{n+1}C_{diff}^{n+1}}\left[V_{am}^{n+1}-R_{bb}^{n+1}\left(I_{F}^{n+1}-I_{rr}^{n+1}\right)\right]=0\\
I_{T}^{n+1}\left(\frac{1}{\Delta t}\right)-I_{T}^{n}\left(\frac{1}{\Delta t}\right)-\frac{1}{L_{ak}}\left(V_{a}^{n+1}-V_{am}^{n+1}\right)=0\\
u_{Cs}^{n+1}\left(\frac{1}{\Delta t}+\frac{1}{R_{damping}^{n+1}C_{S}^{n+1}}\right)-u_{Cs}^{n}\left(\frac{1}{\Delta t}\right)-V_{am}^{n+1}\left(\frac{1}{R_{damping}^{n+1}C_{S}^{n+1}}\right)=0\\
V_{am}^{n+1}=\frac{R_{damping}^{n+1}}{R_{damping}^{n+1}+R_{bb}^{n+1}}\left[V_{ai}^{n+1}+R_{bb}^{n+1}\left(I_{T}^{n+1}+\frac{u_{Cs}^{n+1}}{R_{damping}^{n+1}}\right)\right]\\
V_{a}^{n+1}=\frac{1}{L_{ak}+L_{1}}\left(E_{1}^{n+1}L_{ak}+V_{am}^{n+1}L_{1}\right)\\
I_{F}^{n+1}=IS\left[\exp\left(\frac{q}{kT}V_{ai}^{n+1}\right)-1\right]\\
R_{bb}^{n+1}=\frac{R_{B0}}{\sqrt{1+\frac{I_{F}^{n+1}}{I_{NOM}}}}\\
R_{damping}^{n+1}=DAMPING\sqrt{\frac{L_{ak}}{C_{S}^{n+1}}}\\
C_{diff}^{n+1}=TAU\frac{I_{F}^{n+1}+IS}{M_{0}\cdot\frac{kT}{q}}\\
C_{S}^{n+1}=\begin{cases}C_{0}\cdot[2-e^{-\frac{V_{ai}^{n+1}}{V_{\text{diff}}}})], & V_{ai}^{n+1}\geq 0\\ C_{0}\cdot(\delta-\frac{1-\delta}{(1-\frac{V_{ai}^{n+1}}{V_{\text{diff}}})^{\alpha}}), & V_{ai}^{n+1}<0\end{cases}
\end{cases}
\tag{10}
$$

where the superscripts represent the time levels of the variables. In each time advance, the implicit nonlinear system described by Eqs. (10) needs to be solved by a proper solver. The choice of the nonlinear solver is our focus hereinafter.

2.3 *Fixed-Point and Newton-Type Nonlinear Solvers*

Firstly, for each time advance we reformulate Eqs. (10) as $\mathbf{F}(\mathbf{x}) = \mathbf{0}$, where $\mathbf{x} = [V_{ai},\ I_T,\ u_{Cs},\ \cdots, C_S]^{\mathrm{T}}$ is a column vector holding all unknown variables.

Existing nonlinear solvers can be divided into fixed-point solvers and Newton-type solvers. Many well-known relaxation-based methods, including Jacobi method, Gauss-Seidel method, and successive-over-relaxation (SOR) method, belong to fixed-point solvers. In our context, we divide the unknowns into $\mathbf{x}_1 = [V_{ai},\ I_T,\ u_{Cs}]^{\mathrm{T}}$ and $\mathbf{x}_2 = [V_{am},\ I_F,\ \cdots, C_S]^{\mathrm{T}}$, namely, unknowns explicitly involved in time derivatives are attributed to $\mathbf{x}_1$. The flowchart of the fixed-point method is presented by Fig. 4.

As for Newton-type methods, among which Newton-Raphson (NR) method may be the most famous representative, the essence is to linearize the nonlinear systems and convert the task into a series of linear equations named Newton correction equations, the coefficient matrices of which are the Jacobian matrices of the nonlinear systems at current solutions. These methods usually require explicit evaluation and storage of the Jacobian matrices, which are very costly. Therefore, in this work a new variant of NR method, named the Jacobian-free Newton-Krylov (JFNK) method, is

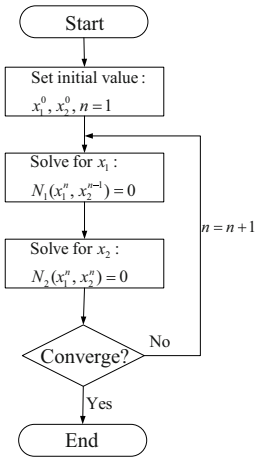

Fig. 4 Flowchart of the relaxation-based fixed-point method [9]

chosen. JFNK method is a nested algorithm consisting of the Inexact Newton (IN) method for the solution of nonlinear equations, and Krylov subspace methods for solving the Newton correction equations. By using the finite difference technique, the matrix-vector products required for Krylov iterations are approximated without forming and storing Jacobian matrices. The readers can refer to [10] for detailed implementations.

3 Numerical Results and Discussions

In this section, the proposed nonlinear solvers are tested on the reference problem. The type of diodes considered here is Infineon D2700U45X122. Firstly, the curves and data from the datasheet are inputted into the device characterization tool integrated in ANSYS Simplorer to extract necessary parameters in the previous equations. The results are given in Table 1, and the simulated transient current and voltage are depicted in Fig. 5.

The diode model and nonlinear solvers are implemented with MATLAB codes. For validation of our implementation, the turn-on process of the diode is analyzed. The total simulation time is 10 ms and the time-step size of MATLAB codes is 0.01 ms. The performance comparison of the nonlinear solvers is shown in Table 2. It's observed that the fixed-point method is obvious faster the JFNK method. Although the average iteration of JFNK method is less than that of the fixed-point method, for each iteration JFNK method demands two evaluations of nonlinear function F(x), which may be the main reason of its lower efficiency. However, for a small portion of the time steps, both methods fail to converge to the desired error tolerance 1E-6 within 100 iterations, which is the predefined maximum number of iterations for each time advance. In this sense, JFNK method is a more robust solver since it fails for fewer time advances.

Table 1 Model parameters extracted using ANSYS Simplorer

Parameter	Explanation	Unit	Value
I_s	Saturation current	A	1.406
M_0	Ideality factor	1	1.188
RB_0	Bulk resistance	Ω	7.796E−4
C_0	Zero voltage junction capacitance	F	1E−7
V_{diff}	Diffusion voltage	V	0.5
α	Capacity exponent	1	0.5
δ	Capacity minimum factor	1	4.089E−4
TAU	Effective lifetime	s	5.358E−7
DAMPING	Relative damping factor	1	2.924
L_ak	Stray inductance	H	2E−7
I_{NOM}	Nominal current	A	2700

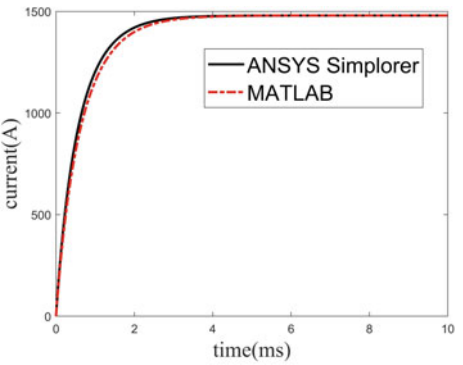

(a) Diode current during the turn-on process.

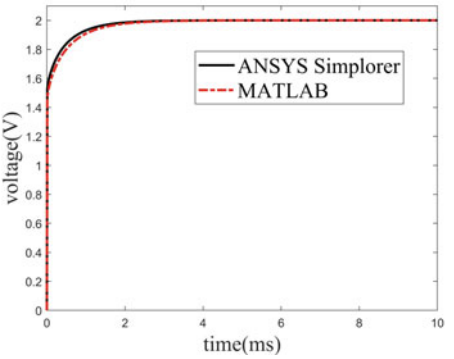

(b) Diode voltage during the turn-on process.

Fig. 5 Transient waveforms of the diode during the turn-on process

Table 2 Performance comparison of the solvers

Indicator	Value	
	JFNK	Fixed-point method
Execution time (s)	47	32
Evaluation of $\mathbf{F}(\mathbf{x})$	40,512	21,984
Number of failed time steps	23	30

When the time-step size is increased to 0.05 ms, it's a totally different story. Fixed-point method fails in most time steps and leads to incorrect waveforms. This is because the convergence of fixed-point methods is pretty sensitive to initial values, and larger time-step size induces more significant difference between current and new-time solution. For comparison, JFNK method fails in 98 time advances yet the waveforms are still acceptable. Nevertheless, the total number of the evaluations of F(x) increased to 62,298 mainly because it takes much more iterations for the inner Krylov solver to converge. Therefore, increased time-step size results in lower efficiency and of course worse accuracy.

4 Conclusions

In this manuscript, a modeling approach requiring merely the manufacturer's datasheet is adopted for transient modeling of power diodes. Then we test two types of nonlinear solvers for resolving the nonlinearity of the diodes. Two conclusions are drawn from the numerical results. Firstly, Newton-type methods are more robust methods, yet they may be less efficient under small time-step size due to the costs for dealing with the Jacobian matrices of the nonlinear systems, either explicitly or implicitly. Secondly, deliberate choice of time-step size is crucial for successful implementations of both types of nonlinear solvers.

Acknowledgements This research is sponsored by the National Natural Science Foundation of Shaanxi Province under Grant 2022JQ-484, and the state key laboratory of electrical insulation and power equipment, Xi'an Jiaotong University under grant EIPE21302.

References

1. Yuan, L., Meng, Q., Zhao, W., et al.: Study of the switching characteristic of power diode in the high power inverter. Power Electron. **50**(9), 106–108 (2016). (in Chinese)
2. Jia, S., Zhao, Z., Shi, B., et al.: Numerical modeling and analysis of electromagnetic interference in power electronics systems. Trans. China Electrotechnical Soc. **36**(11), 2383–2393 (2021). (in Chinese)

3. Oliveira, R., Yazdani, A.: A modular multilevel converter with DC fault handling capability and enhanced efficiency for HVDC system applications. IEEE Trans. Power Electron. **33**(1), 11–22 (2018)
4. Benigni, A., Monti, A., Dougal, A.: Latency-based approach to the simulation of large power electronics systems. IEEE Trans. Power Electron. **29**(6), 3201–3213 (2014)
5. Hui, S., Fung, K.: Fast decoupled simulation of large power electronic systems using new two-port companion link models. IEEE Trans. Power Electron. **12**(3), 462–473 (1997)
6. Zhu, R., Lin, N., Dinavashi, V., et al.: An accurate and fast method for conducted EMI modeling and simulation of MMC-based HVDC converter station. IEEE Trans. Power Electron. **35**(5), 4689–4701 (2020)
7. Lin, N., Zhu, R., Dinavashi, V.: Hierarchical device-level modular multilevel converter modeling for parallel and heterogeneous transient simulation of HVDC systems. IEEE Open J. Power Electron. **1**, 312–321 (2020)
8. Zhu, R., Huang, Z., Dinavashi, V.: A universal wideband device-level parallel simulation method and conducted EMI analysis for more electric aircraft microgrid. IEEE J. Emerg. Sel. Top. Ind. Electron. **1**(2), 162–171 (2020)
9. Wang, J., Chen, F., Ma, X.: A hybrid indirect-direct coupling method for strongly coupled nonlinear magnetic problems. IEEE Trans. Magn. **53**(8), 7207611 (2017)
10. Knoll, D., Keyes, D.: Jacobian-free Newton-Krylov methods: a survey of approaches and applications. J. Comput. Phys. **193**(2), 357–397 (2004)